Adaptive Balancing Strategy for Cell Capacitor Voltage in a Modular Multilevel Converter

Sheik Hussain[1], **Roma Raina**[1],
Hidayathullah Mohamed Ismail[2†], and **Saravanan Kaliyaperumal**[2], Non-members

ABSTRACT

Due to the modular structure and voltage scalable features, the Modular Multilevel Converter (MMC) has become an alternative converter for high and medium voltage-based transmission systems. Apart from this, MMC has edible features in controlling the real and reactive power for a high-voltage transmission system compared to the conventional converter. However, some of the technical challenges such as control complexity when subjected to more voltage levels, capacitor voltage balancing issues, increase in capacitor voltage ripples, DC fault handling, and circulating current affect the performance of MMC in various applications. In this paper, an adaptive balancing strategy is proposed for capacitor voltage balancing of each cell connected in the MMC. This approach balances the floating capacitor in a simplified manner and henceforth reduces the capacitor voltage ripples to the permissible limit. In addition, the circulating current present in the MMC circuit will be suppressed in comparison to the conventional method. The proposed strategy is investigated under various operating conditions to analyze the effective performance compared to the traditional technique. A comparative study of the proposed approach is presented with various parameters of MMC performed using MATLAB Simulink software.

Keywords: Adaptive Balancing Strategy, HVDC Applications, Modular Multilevel Converter, Capacitor Ripple Voltage Control

1. INTRODUCTION

The Modular Multilevel Converter (MMC) has become an important research idea among industries and academicians after being first installed by Siemens in 2010 in California (United States of America). However, initially, the MMC was developed for a high-voltage transmission system [1], then extended to other applications such as power quality [2], variable speed drives [3], electric traction systems [4], and multi-terminal systems [5]. Furthermore, due to the advancement in semiconductor devices, multi-control variable controller, and the signal conditioning process, the MMC has been further extended to renewable energy (offshore wind plant) [2, 6] and microgrid [7] applications. The main technical challenges associated with consistent operation of the MMC include capacitor voltage balancing, capacitor ripple mitigation, output current control, and arm voltage control. During the past decades, many academicians have started to develop various control functions for regulating the technical challenges of MMC.

Among them, the most important features of MMC include modular construction, voltage scalability, low voltage-rated cell connected in stacked phases, low harmonic distortion, and the ability to work during fault conditions. However, despite its several advantages, the reliable operation of the MMC is affected by the capacitor ripple voltage, circulating current, voltage, and power fluctuation due to uneven voltage balancing and increased power loss. The switching and control operation of the MMC mainly depends upon the selection of a suitable cell topology [8, 9]. Many cell topologies are available for the MMC, with half bridge and full bridge commonly used for real-time applications [10].

In order to select a suitable topology for the MMC, a comparative analysis is performed based on the number of power devices required, power loss, and harmonic performance, as illustrated in Fig. 1. The different cell types are half bridge (HB), full bridge (FB), clamp double (CD), neutral point clamp (NPC), flying capacitor (FC), hybrid, mixed, and T type NPC. Each cell consists of numerous switching devices and capacitors in each arm of the converter. Furthermore, the charging and discharging of each cell capacitor voltage mainly depend upon the voltage balancing method. However, due to the uneven balancing effects, the peak ripple of the capacitor voltage and circulating current will be high, henceforth increasing the power loss and reducing the efficiency of the MMC. Hence, balancing the capacitor voltage to its nominal value is an important MMC phenomenon.

Over the past decade, many capacitor-balancing techniques have been developed to balance the capacitor voltage with respect to the rated quantity [11]. Consequently, the self-voltage balancing technique is used to

Manuscript received on April 20, 2022; revised on June 17, 2022; accepted on July 7, 2022. This paper was recommended by Editor-in-Chief Yuttana Kumsuwan.

[1]The authors are with the Department of Energy System Management, Manipal Academy of Higher Education, Dubai, The United Arab Emirates.

[2]The authors are with the Department of Electrical and Electronics Engineering, SRM Institute of Science and Technology, Kattankulathur, Tamil Nadu, India.

[†]Corresponding author: hidayathullahm@googlemail.com

Digital Object Identifier: 10.37936/ecti-eec.2023211.248601

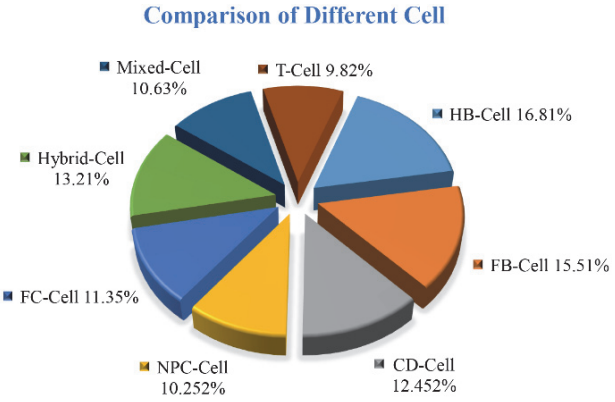

***Fig. 1**: Comparison of different cell topologies.*

regulate the capacitor voltage using modulation schemes such as nearest level [12], space vector [13], carrier phase shift [14], and multicarrier [15]. Besides, these techniques require an additional control method for mitigating the peak ripple voltage of each cell capacitor while also increasing power loss in the converter. In order to overcome these problems, a novel modulation scheme with voltage control algorithm is developed to balance the capacitor voltage [16], but it affects the efficiency and increases the cost of the MMC.

Apart from this, various voltage sorting-based balancing methods have been developed to balance the cell capacitor using the novel balancing method [17]. These techniques use the voltage band process to select each cell capacitor voltage using the maxima and minima functions. However, the voltage band selection process requires more computation time while also increasing the system's complexity. Furthermore, an additional controller is needed when the MMC is subjected to a large number of cells. This is overcome by using modified voltage balancing techniques [18] but increases the circulating current and power loss in the MMC. Besides, many control algorithms based on injecting the circulating current [19] have been developed to mitigate the capacitor ripple voltage and voltage fluctuation caused during steady state and dynamic conditions.

These regulate the ripple voltage and balance the capacitor voltage with even distribution. However, they cause a sudden voltage deviation under abnormal conditions in the load terminal, eventually increasing conduction loss, harmonic distortion, and circulating current. This problem is overcome by using modulation-based balancing techniques [20], where the centralized controller is employed for balancing each cell capacitor. However, it increases the switching transition and makes the system more complex when the number of cells is increased. Thus, the aforementioned techniques have several limitations in controlling the voltage of each cell capacitor and regulating the capacitor ripple voltage.

Hence, to overcome the problem associated with the conventional techniques, a simplified control algorithm is required to balance each capacitor voltage. Furthermore, it must mitigate the peak ripple voltage and circulating current toward the acceptable limit for the MMC.

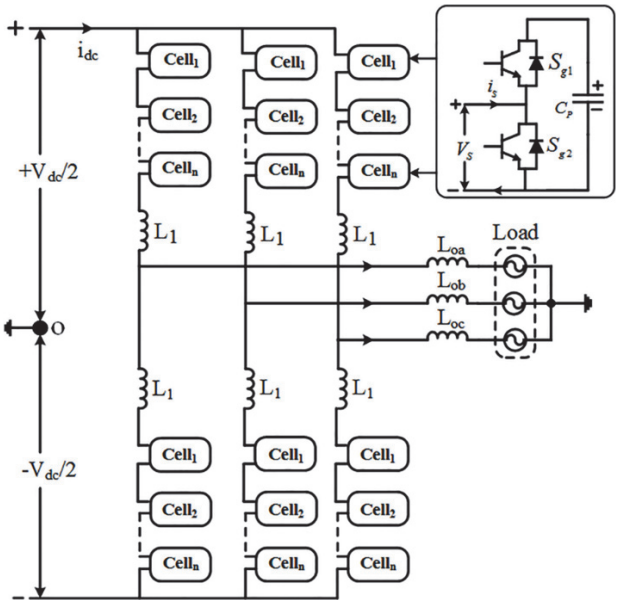

***Fig. 2**: Generalized configuration of the MMC.*

Based on the above mentioned problems, an adaptive balancing strategy is proposed to balance each cell capacitor. Furthermore, the proposed method will also regulate the ripple voltage and circulating current to the permissible limit compared to the traditional method. Phase disposition is used to generate the pulse in the proposed method. Simulation and comparative analysis are carried out to understand the performance of the proposed balancing method.

2. GENERALIZED CONFIGURATION OF THE MMC

The generalized configuration of the MMC with HB cell (based on Fig. 1) topology is shown in Fig. 2. The three-phase MMC structure consists of an input DC link source (V_{dc}), upper and lower arm, arm inductor (L_0), and three-phase (R, Y, and B) load, as depicted in Fig. 2. The upper and lower arms consist of an N number of series connected cells, with each cell consisting of two identical switching devices (S_{g1} and S_{g2}) (where the antiparallel diodes are connected across each switch) and the floating capacitor (C_P). The most widely used topology for the MMC is the HB cell [1], because of its simple structure, reduced power loss, and ease of control.

In addition, DC fault handling can be attained by connecting the redundant cells in the converter [21]. The arm inductor connected at the midpoint of the upper and lower arm is used to control the instantaneous voltage changes during modulation and supresses the circulating current. The single HB cell generates two output voltage levels 0 (when S_{g2} is in ON condition) and $+V_C$ (when S_{g1} is in the ON condition). The complete switching operation of a single HB cell is depicted in Table 1. The

***Table 1**: Switching sequence of the HB cell.*

Switches in Conduction		Arm	Capacitor	Output
S_{g1}	S_{g2}	Current	Condition	Voltage
off	off	> 0	Charging	$+V_C$
off	on	> 0	Bypass	0
on	off	< 0	Discharging	$-V_C$
off	on	< 0	Bypass	0

main control objectives of the MMC are the number of output voltage levels, arm and output current control, harmonic performance, and capacitor ripple reduction. These control functions can be carried out based on the proper switching of the power devices connected in the MMC. The three-phase output depends upon the number of voltage levels generated and appropriate modulation techniques used in the switching process.

3. MATHEMATICAL MODEL

The main control parameters of the MMC include arm voltage, circulating current, input DC voltage, output voltage, and current. The arm voltage directly depends upon the voltage of each cell because of its cascaded connection. Hence, to understand each control function of the MMC for theoretical analysis, the basic structure is converted into an equivalent circuit model (due to its simplicity and ability to control multi-variables [22, 23]).

Consequently, each arm of the MMC is converted into a controlled voltage source while the arm resistance is included to analyze the power in each arm. Similarly, the resistive and inductive load considered for analyzing the performance of the proposed method is considered in the theoretical analysis. Additionally, important parameters affecting the stability of the MMC are capacitor ripple voltage and circulating current. The circulating current is caused by sudden changes in the capacitor voltage due to the switching function. However, the current does not affect the root mean square (RMS) value of the output but increases the peak magnitude of the arm current. This results in increased power loss between each cell connected in the MMC.

The steady state and dynamic conditions of each control parameter of the MMC are analyzed based on the application of Kirchhoff's voltage law in each arm. Consequently, the output voltage obtained at the midpoint of the MMC is determined as,

$$V_{Lx}=\frac{V_{dc}}{2}+V_{ux}+L_1\frac{di_{ux}}{dt}+R_1i_{ux}+L_0\frac{di_{0x}}{dt}+R_0i_{0x}+V_{rx} \tag{1}$$

$$V_{Lx}=\frac{V_{dc}}{2}+V_{lx}+L_1\frac{di_{lx}}{dt}+R_1i_{lx}+L_0\frac{di_{0x}}{dt}+R_0i_{0x}+V_{rx} \tag{2}$$

where $V_{ux} = V_{ua} + V_{ub} + V_{uc}$, $V_{lx} = V_{la} + V_{lb} + V_{lc}$, $V_{ua} = V_{ub} = V_{uc} = nV_C$, and $V_{la} = V_{lb} = V_{lc} = nV_C$. V_{Lx} represents the output voltage obtained at the midpoint, V_{ux} and V_{lx} denote the upper and lower arm voltage, R_1 and L_1 are the arm resistor and inductor, R_0 and L_0 imply the load resistance and inductance, and V_{0x} and i_{0x} are the load voltage and current of each phase. Likewise, the upper and lower arm current is determined by,

$$\begin{aligned} i_{ux} &= \frac{1}{2}\left(i_{acx}+i_{dc}\right)+i_{clx} \\ i_{lx} &= \frac{1}{2}\left(i_{acx}-i_{dc}\right)+i_{clx} \end{aligned} \tag{3}$$

i_{ux} and i_{lx} represent the upper and lower arm current, x represents phase R, Y and B, while i_{cl} denotes the circulating current. Furthermore, the input DC voltage is expressed as,

$$V_{dc}=V_{ux}+V_{lx}+L_1\frac{d\left(i_{ux}-i_{lx}\right)}{dt}+R_1\left(i_{ux}-i_{lx}\right) \tag{4}$$

Thus, by equating Eq. (1) and Eq. (2) with respect to DC voltage, it can be modified as,

$$\begin{aligned} V_{dc} = V_{ux}-V_{lx}+L_1\frac{d\left(i_{ux}+i_{lx}\right)}{dt}+R_1\left(i_{ux}+i_{lx}\right) \\ +2L_0\frac{di_{0x}}{dt}+2R_0i_{0x}+2V_{rx} \end{aligned} \tag{5}$$

Likewise, the load current and input DC current is expressed as,

$$i_{0x}=i_{0a}+i_{0b}+i_{0c} \tag{6}$$

$$i_{dc}=\frac{i_{ux}-i_{lx}}{6} \tag{7}$$

The dynamic variation of input DC current is determined by,

$$\frac{di_{dc}}{dt}=\frac{\frac{V_{dc}}{2}-\left(\frac{V_{ux}-V_{lx}}{6}\right)+L_0\frac{di_{0x}}{dt}+R_1i_{dc}+R_0\frac{i_{0x}}{3}+\frac{V_{rx}}{3}}{3L_1} \tag{8}$$

In addition, the circulating current flowing in each arm of the converter is determined by,

$$i_{cl}=\left(\frac{i_{ux}-i_{lx}}{2}\right)-i_{dc} \tag{9}$$

The dynamic condition of the circulating current in the converter is determined by,

$$\frac{di_{clx}}{dt}=\frac{\left(\frac{V_{ux}-V_{lx}}{6}\right)-\left(\frac{V^u_{Lx}+V^l_{Lx}}{2}\right)-R_0i_{cl}}{L_1} \tag{10}$$

Likewise, in some case the presence of a common mode current (motor drive) can be obtained by,

$$i_{cm} = \frac{i_{ux} + i_{lx}}{6} \tag{11}$$

In similarity to the DC current, the dynamic condition of the common mode current (i_{cm}) is determined by differentiating Eq. (11),

$$\frac{di_{cm}}{dt} = \frac{-V_{ux} + V_{lx} - 2L_0\frac{di_{0x}}{dt} - 2R_0 i_{0x} - 2V_{rx}}{6L_1} \tag{12}$$

Thus, while considering the load parameters, Eq. (12) is once again modified into,

$$\frac{di_{cm}}{dt} = \frac{\left(\frac{V_{lx} - V_{ux}}{6}\right) - \left(2R_0 + 3R_1\right) i_{0x}}{L_1 + 3L_0} \tag{13}$$

Additionally, the relationship between the load current and common mode current is determined as,

$$i_{0x} = \frac{1}{2}\left(i_{ux} + i_{lx}\right) - i_{cm} \tag{14}$$

The dynamic changes that occur during abnormal conditions in the load behavior based on the load current are determined as,

$$\frac{di_{0x}}{dt} = \frac{1}{2L_0}\left[\left(\frac{V_{lx}^{l} - V_{ux}^{u}}{6}\right) - V_{rx} - 2\left(R_0 + R_1\right) i_{0x}\right] \tag{15}$$

The power loss in the converter can be determined by calculating the input and output power flowing in the arm side as well as the load side can be determined by,

$$P_{int} = P_{out} + P_{loss} \tag{16}$$

$$V_{dc} I_{dc} = \left(V_{ux} i_{ux} + V_{lx} i_{lx}\right) + P_{loss} \tag{17}$$

$$P_{loss} = V_{dc} i_{dc} - \left(V_{ux} i_{ux} + V_{lx} i_{lx}\right) \tag{18}$$

where P_{int} denotes the input power loss, P_{out} represents the output power loss, and P_{loss} denotes the switching and conduction loss. Hence, the theoretical analysis of the MMC is discussed in detail in this section. The dynamic analysis based on the sudden change in load quantities during abnormal conditions is evaluated for arm voltage, circulating current, output current, and common mode current. Thus, based on this analysis the steady state and dynamic changes of the MMC can be determined using the equivalent circuit model.

4. PROPOSED ADAPTIVE BALANCING STRATEGY

The important factor to be considered for steady and consistent operation of the MMC includes a suitable pulse generation scheme for switching the power devices and capacitor-balancing algorithm.

4.1 Pulse Generation Scheme

Pulse generation is nothing but a signal used to trigger the semiconductor devices in any power converter. The pulse signal generation is generally obtained by comparing the reference sinusoidal with the triangular carrier signal. Based on the carrier arrangement, the pulse generation techniques are classified into many types such as selective harmonics elimination, space vector modulation, nearest level, phase shift carrier, and level shift carrier [15]. Of these, the level shift carrier technique is most widely used for the MMC due to its superior harmonic performance and low power loss [24]. Furthermore, the level shift carrier technique is classified into PD (phase disposition), APOD (alternate phase opposition disposition), and POD (phase opposition disposition). The PD pulse generation technique is used for the proposed balancing operation, as illustrated in Fig. 3.

In that respect, the sinusoidal signal is compared with the carrier signal, where each carrier signal is organized in vertical arrangement with equal disposition at each level. Fig. 3(a) represents the pulse generation pattern of the power devices while Fig. 3(b) represents the desired output voltage determined at the load terminal of the MMC. In order to understand the performance of the MMC, the number of cells for the proposed method is selected as 4 per arm. Hence, four carrier signals are required in the adaptive technique. The number of levels generated at the output of the converter can be determined by,

$$N_{level} = N_C + 1 \tag{19}$$

where N_{level} represents the number of levels and N_C denotes the number of cells. Likewise, the reference signal generated for each arm voltage of the MMC can be obtained by,

$$V_{aup}^{ref} = \frac{V_{dc}}{2}\left[1 - \left(M_I * \sin\omega t\right)\right]$$
$$V_{alp}^{ref} = \frac{V_{dc}}{2}\left[1 + \left(M_I * \sin\omega t\right)\right] \tag{20}$$

4.2 Adaptive Balancing Strategy

Voltage balancing at each cell capacitor is the primary control objective of the modular-based high-power converter. Furthermore, it also plays an important role in the steady and consistent operation of the MMC. The basic function of the cell capacitor is used to charge and discharge the voltage to the nominal value. However, balancing each capacitor voltage to the nominal value is quite a challenging task due to the presence of a large number of cells in the MMC. Therefore, an edible capacitor-balancing technique is required to balance each cell voltage, each of which must be balanced evenly at each voltage level. Hence, an adaptive balancing strategy is developed in this study to control each cell

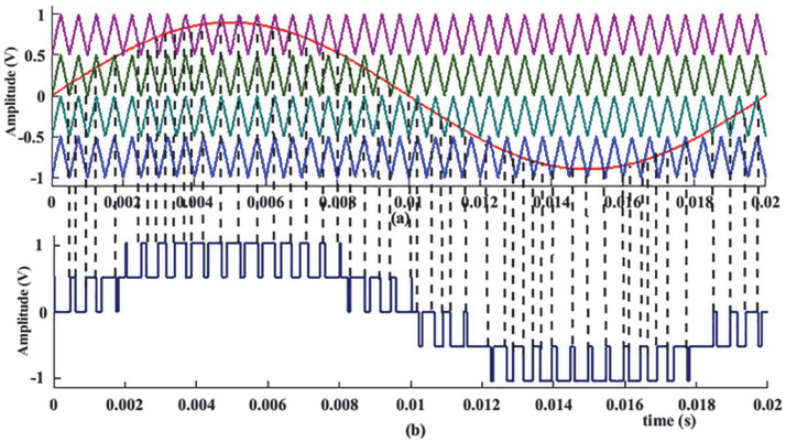

Fig. 3: Pulse generation using the PD technique.

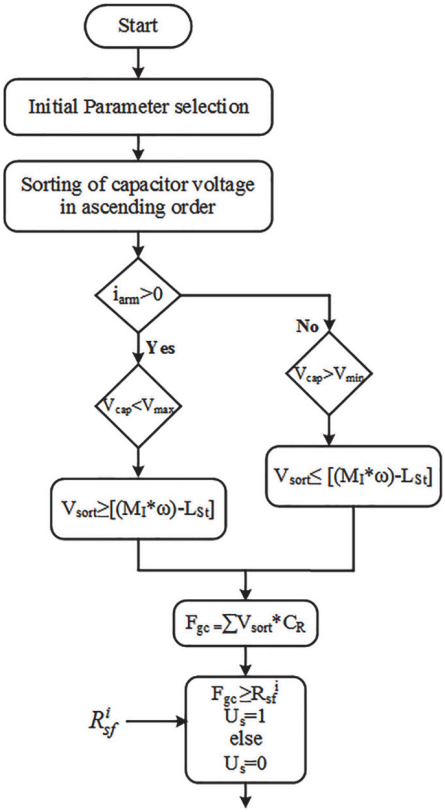

Fig. 4: Adaptive balancing strategy.

capacitor voltage as well as regulating the capacitor ripple voltage toward the permissible limit. Initially, each capacitor voltage is selected based on the sorting mechanism developed by [25]. The capacitor voltage is selected by the highest to lowest values using the bubble sort technique [20].

Hence, the required capacitor voltage is selected for the proposed adaptive technique. Furthermore, it requires the switching pulse signal, obtained using the PD pulse generation scheme (as discussed in the previous section). The control algorithm of the proposed adaptive balancing strategy is illustrated in Fig. 4. After the selection of each capacitor voltage and pulse signal from the PD technique, the operating conditions of capacitor voltage (charging and discharging) are calculated based on the arm current direction (i_{arm}). Furthermore, the switching sequence for the charging and discharging is determined according to Table 1. Based on the switching sequence of the HB cell, the required capacitor voltage is selected, by comparing the maximum (V_{max}) and minimum (V_{min}) conditions.

Thus, the obtained capacitor voltage is incorporated with the switching signal (L_{St}) and modulation index (M_I) values. Based on that, the required capacitor-sorted voltage (V_{sort}) is determined, which is expressed by,

$$\begin{aligned} V_{sort} &\geq \left(M_I * \omega t\right) - L_{St} \\ V_{sort} &\leq \left(M_I * \omega t\right) - L_{St} \end{aligned} \tag{21}$$

However, the obtained V_{sort} is regulated with two conditions, one is when $V_{cap} < V_{max}$ and the charged capacitor voltage is then selected, and another is when $V_{cap} > V_{max}$ in which case the discharged capacitor voltage is selected. The selected V_{sort} signal is once again compared with the carrier rotation (C_R) signal as proposed by [9].

Based on the comparison, the gate function (F_{gc}) is determined. This comparative process is used to increase the delay time and to regulate the ripple voltage in each cell. Thus, the obtained signal can be given as an input to the power device in each cell of the MMC. Since the MMC consists of a large number of cells connected in each arm, the obtained F_{gc} signal cannot be incorporated into more cells due to the control complexity. Furthermore, the signal may get overlapped during the switching function. Hence, in order to increase the delay time constant for each switching device when subjected to more cells, the reference switching signal (R_{sf}^i) is compared with the F_{gc} to determine the required switching pulse signal (U_s) for the MMC. The same process can be performed on many cells without any changes in the switching

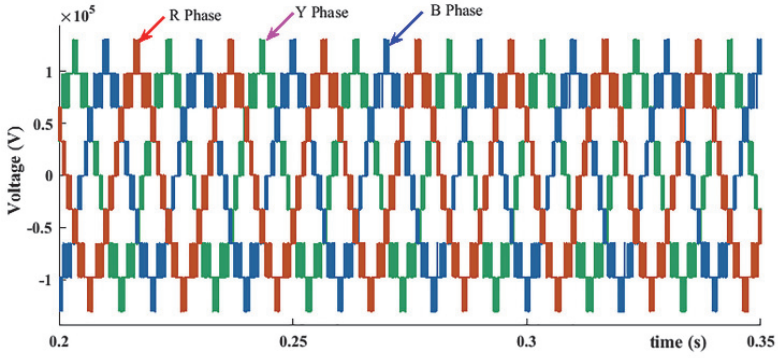

Fig. 5: Three-phase voltage waveform.

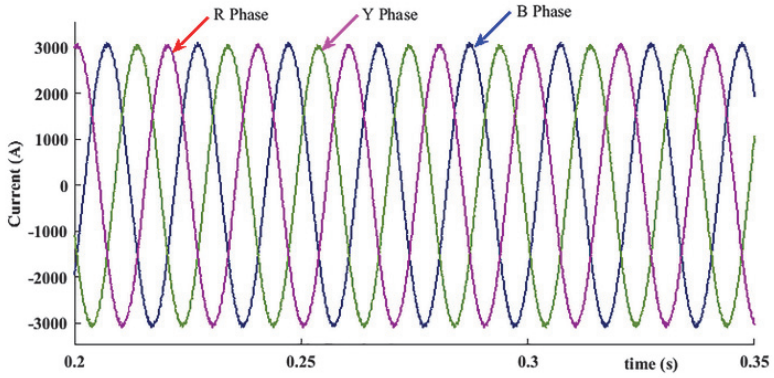

Fig. 6: Three-phase current waveform.

Table 2: Simulation parameter values.

Parameters Values	Simulation
Output Power	350 MW
Grid Voltage	132 kV
Output current	3 kA
DC Link	190 kV
Source Inductance	20 mH
Source Resistance	0.01 Ω
Number of SM	4
Cell Capacitance	3 mF
Load Resistance	23 Ω
Load Inductance	30 mH
F_{sw}	2.5 kHz
Modulation Index	0.95

function. Thus, the signal U_s provides the required pulse signal for the MMC.

5. SIMULATION RESULTS

The effective performance of the proposed adaptive balancing strategy is tested in the MATLAB/Simulink software tool. The source and load (resistance and inductance) values required for testing the proposed method in the MMC are depicted in Table 2. The modulation index and switching frequency (F_{sw}) for PD modulation of the MMC are selected as 0.95 and 2.5 kHz, respectively. Based on the analysis, the desired outputs such as three-phase line voltage and current, capacitor voltage, phase voltage, and real power quantities are evaluated using the proposed method.

Fig. 5 presents the three-phase output voltage characteristics of the MMC obtained at its midpoint (as in Fig. 1). Since the number of cells determined for the proposed method is 4 per arm, it generates a five-level voltage at the output. For simplification, the number of cells required in each arm is selected as 4, but in a practical system, it will be more (for example, more than 100 cells per arm). Furthermore, in a real-time study, the selection of the number of cells, capacitors, and power devices is based on the power rating, application, and operating limit. Likewise, the selection of a typical capacitor for the MMC is an important phenomenon. The selection of capacitor and inductor values for the MMC is explained in detail in [26], and the various practical applications discussed.

Consequently, the capacitor and inductor values are selected for the proposed method. The output voltage magnitude of 132 kV is attained at the load terminal. Hence, according to Fig. 5, each voltage level indicates that the proposed technique balances the capacitor voltage at equal distribution. Similarly, the characteristics of the output current curve are illustrated in Fig. 6.

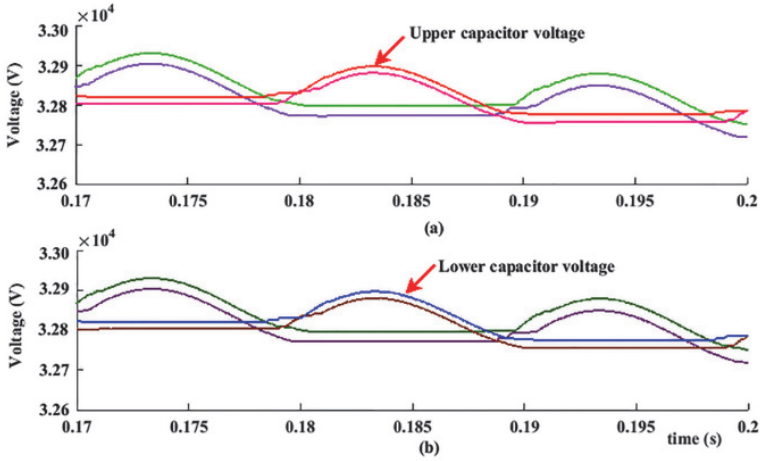

Fig. 7: 4-cell capacitor voltage (upper and lower).

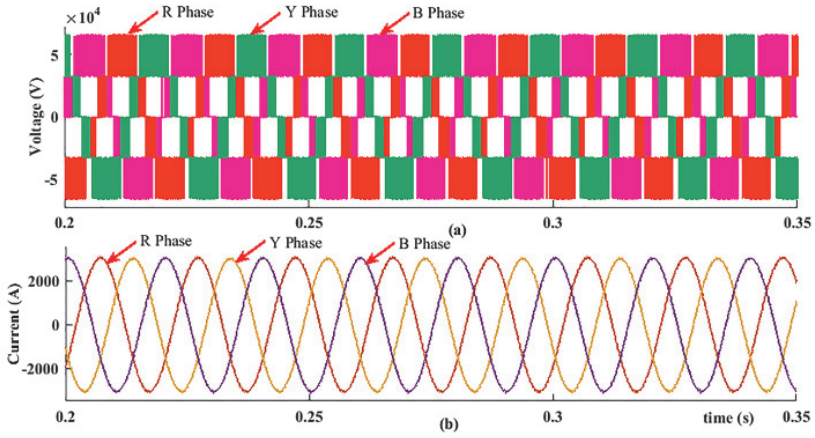

Fig. 8: Phase voltage of R, Y, and B.

A near to sinusoidal signal is achieved at the output terminal with fewer DC and AC harmonic components. In the case of the MMC, the presence of low-order harmonics tend to be higher compared to others, due to uneven voltage distribution and the circulating current. The cell capacitor voltage of the upper and lower arm of the R phase is depicted in Fig. 7. Each cell capacitor voltage is balanced at the rate of 33.28 kV (i.e., 25% of the nominal value).

As can be observed from Fig. 7, each cell capacitor voltage is balanced evenly without any deviation. Similarly, peak-to-peak magnitude is obtained as 125 V (ripple voltage). Hence, the proposed adaptive balancing strategy balances the capacitor voltage with equal voltage distribution.

The phase voltage and current (each line to ground) of the MMC are shown in Fig. 8, depicting the effectiveness of the proposed adaptive balancing strategy. Likewise, the arm voltage and current of the R phase are depicted in Figs. 9 and 10.

The arm quantities play a vital role in the steady and consistent operation of the MMC because the instantaneous voltage changes in each cell due to the switching device determined in each arm of the converter. Hence, if any disturbance occurs during the switching function, it will directly impact the arm voltage and current, eventually affecting the stability of the MMC while increasing power loss.

From Figs. 9 and 10, it can be concluded that the proposed method maintains the voltage and current with nominal values without any disturbance. Until now, the proposed method is tested in fixed load conditions ($R_L = 15\,\Omega$ and $L_L = 20$ mH) with the modulation index and F_{sw} at 0.95 and 2.5 kHz, respectively.

Furthermore, in order to understand the performance of the adaptive balancing techniques in dynamic conditions, the step change in load values is incorporated at the midpoint of the MMC in equal time intervals. On that basis, the performance of load voltage, current, and capacitor voltage is measured. Initially, the converter is tested in half load conditions from the time period of 0 to 0.16 s, after which the step change to full load

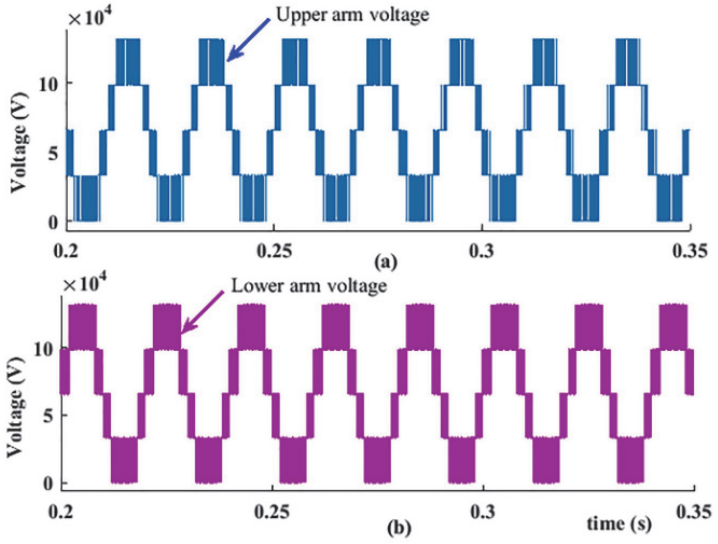

Fig. 9: Arm voltage.

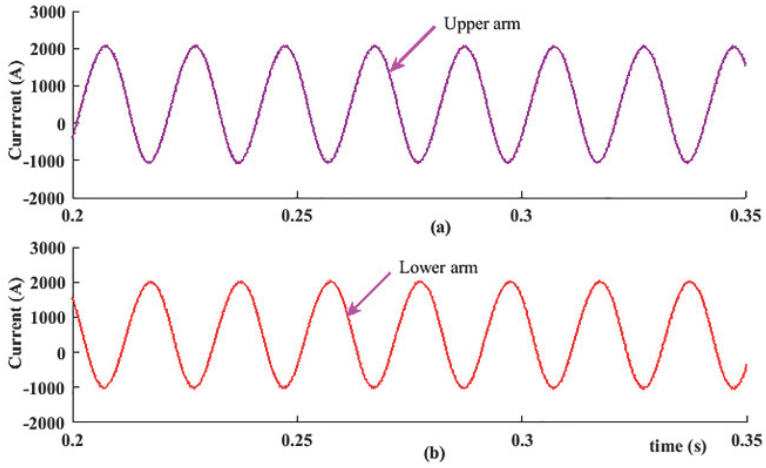

Fig. 10: Arm current.

conditions is incorporated from 0.17 s. The output voltage and current characteristic curve during dynamic load conditions are illustrated in Fig. 11.

Fig. 11(a) depicts the output voltage while Fig. 11(b) shows the load current waveform. This depicts that, during half load and full load conditions, the adaptive balancing strategy performs quite well in terms of balancing each capacitor voltage at each voltage level, as shown in Fig. 12(a).

Besides, during dynamic load conditions, the current is increased from 2.5 kA to 5 kA of the rated value. During these load conditions, the output current attains near to the sinusoidal signal without any harmonics present in the peak current magnitude. Similarly, when considering each cell capacitor voltage, during the step load variation the capacitor is evenly balanced without any deviation, as depicted in Fig. 12. However, during dynamic conditions, there may be a slight increase in the peak-to-peak value of each cell capacitor. Apart from this, the proposed method balances each cell capacitor to their nominal values.

Likewise, in order to validate the real power flowing through the MMC during dynamic conditions, the characteristic curve of the real power flowing in the MMC is illustrated in Fig. 13. As Fig. 13 clearly indicates, during dynamic conditions only the real power values are varied from half load to full load without any deviation. Likewise, the reactive power flow during dynamic load conditions is shown in Fig. 14.

Hence, according to the simulation results, the effective performance of the adaptive balancing strategy is validated under various operating conditions. Furthermore, in order to understand the performance of the proposed method with other balancing techniques, a comparative analysis is carried out based on the different parameters such as capacitor ripple, circulating current, voltage harmonics (THD_v), current harmonic distortion (THD_i), power loss, and complexity of the MMC. Based

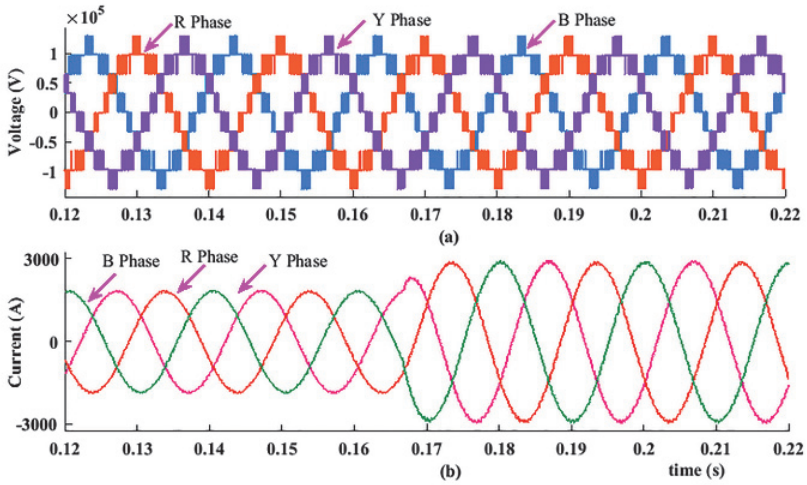

Fig. 11: Three-phase quantities (dynamic load variation).

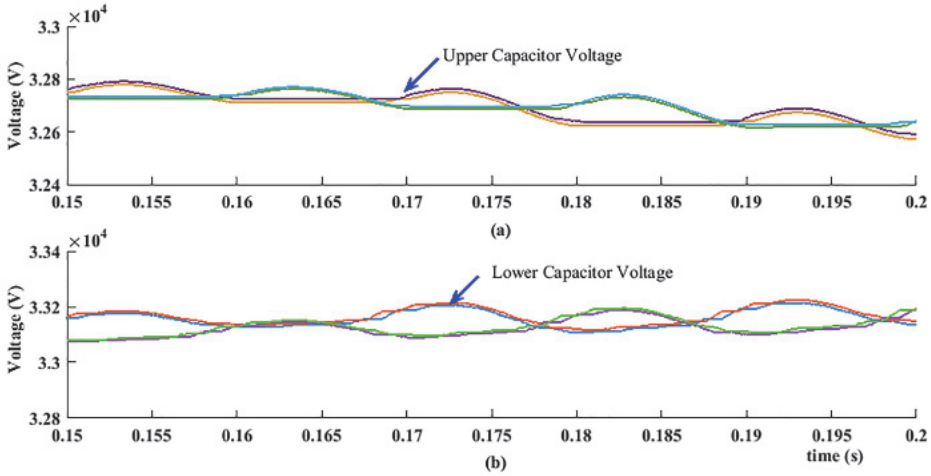

Fig. 12: Capacitor voltage under dynamic load conditions.

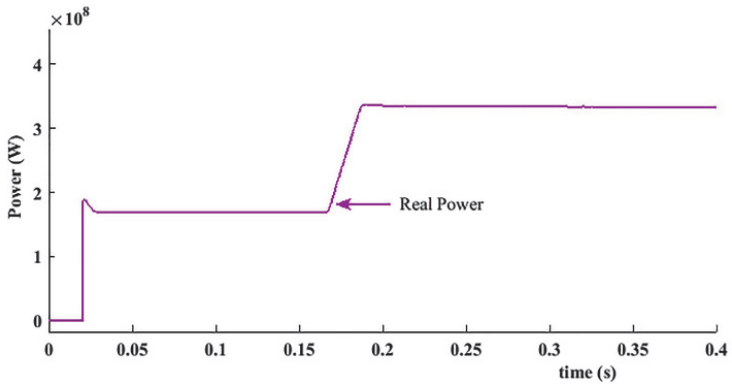

Fig. 13: Real power waveform.

on the findings of the study, the proposed adaptive balancing strategy performs quite well compared to other traditional techniques. The measured values are shown in Table 3. It should be noted that the number of cells selected for the proposed method is 4 with a rated voltage of 132 kV. Hence, the capacitor voltage attained at the output of each cell is 25% (33 kV) of the rated voltage. Similarly, this also applies to power device selection.

In practice, the same process cannot be followed because, in a modular converter, there will be more

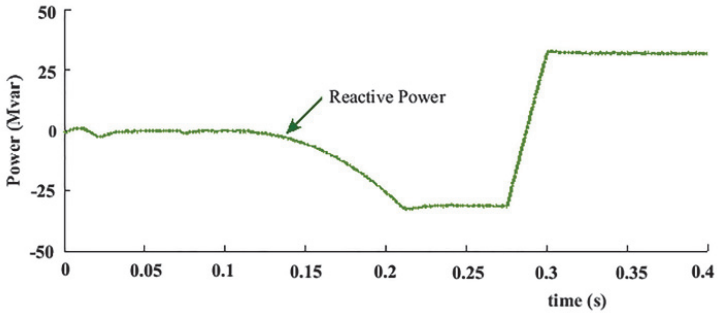

***Fig. 14**: Real power waveform.*

***Table 3**: Comparative analysis of the proposed method vs traditional techniques.*

Ref.	Cell	Capacitor Ripple (V)		Circulating Current (A)	Capacitor Ripple (V)	THD_v (%)	THD_i (%)	Control Complexity	Power Loss (kW)
		Half Load	Full Load						
[8], [12]	HB	135	153	60.23	153	22.32	8.96	High	9.65
[13], [15]	FC	189	196	37.69	196	26.83	9.52	Low	5.21
[18]	FB	145	156	78.9	156	32.32	12.59	High	4.8
[22], [24]	HB	156	175	38.63	175	26.23	11.95	Moderate	6.21
Proposed	HB	112	125	27.65	125	19.78	7.65	Low	3.98

cells. However, the aim of this study is to analyze the performance of the proposed method with a simple model. However, in practical application, the same procedure can be followed for a higher number of cells without much modification to the balancing method.

6. CONCLUSION

This paper discusses the performance efficiency of the adaptive balancing strategy for balancing each cell capacitor voltage in the MMC. The HB is used as the cell topology for the steady and consistent operation of the MMC. Furthermore, the phase disposition technique is used as a pulse signal generation pattern for the switching devices in each cell. The obtained pulse signal and capacitor voltage are given as inputs to the control algorithm to manipulate the balancing function. Based on the adaptive function, the desired pulse signal for the MMC is generated at the output of the control algorithm, henceforth given as an input to the MMC. Moreover, the adaptive technique balances each cell capacitor with equal distribution while also regulating the peak ripple voltage of the capacitor. In addition, a comparative analysis is carried out with the other conventional techniques, to evaluate the performance effectiveness of the proposed method. The findings reveal that the performance of the proposed balancing techniques is quite good compared to other methods in terms of capacitor ripple, harmonics, power loss, and control complexity. Since the MMC is widely used mostly for high-voltage systems. The performance of the proposed method is tested using a high-voltage application in the MATLAB/Simulink environment.

REFERENCES

[1] A. Lesnicar and R. Marquardt, "An innovative modular multilevel converter topology suitable for a wide power range," in *2003 IEEE Bologna Power Tech Conference Proceedings*, vol. 3, Bologna, Italy, 2003.

[2] G. Guo *et al.*, "Series-connected-based offshore wind farms with full-bridge modular multilevel converter as grid- and generator-side converters," *IEEE Transactions on Industrial Electronics*, vol. 67, no. 4, pp. 2798–2809, Apr. 2020.

[3] A. K. Hannan and T. K. Hassan, "Design and simulation of modular multilevel converter fed induction motor drive," *Indonesian Journal of Electrical Engineering and Informatics (IJEEI)*, vol. 9, no. 1, pp. 22–36, Mar. 2021.

[4] M. Tanta *et al.*, "Experimental validation of a reduced-scale rail power conditioner based on modular multilevel converter for AC railway power grids," *Energies*, vol. 14, no. 2, 2021, Art. no. 484.

[5] L. Zhang *et al.*, "Modeling, control, and protection of modular multilevel converter-based multi-terminal HVDC systems: A review," *CSEE Journal of Power and Energy Systems*, vol. 3, no. 4, pp. 340–352, Dec. 2017.

[6] S. Haq, S. P. Biswas, M. K. Hosain, M. A. Rahman, M. R. Islam, and S. Jahan, "A modular multilevel converter with an advanced PWM control technique for grid-tied photovoltaic system," *Energies*, vol. 14, no. 2, 2021, Art. no. 331.

[7] Q. Xiao *et al.*, "Novel modular multilevel converter-based five-terminal MV/LV hybrid AC/DC microgrids with improved operation capability under

unbalanced power distribution," *Applied Energy*, vol. 306, Jan. 2022, Art. no. 118140.

[8] Y. Tian, H. R. Wickramasinghe, Z. Li, J. Pou, and G. Konstantinou, "Review, classification and loss comparison of modular multilevel converter submodules for HVDC applications," *Energies*, vol. 15, no. 6, 2022, Art. no. 1985.

[9] H. M. Ismail and S. Kaliyaperumal, "Enhanced voltage sorting algorithm for balancing the capacitor voltage in modular multilevel converter," *IEEE Access*, vol. 9, pp. 167 489–167 502, 2021.

[10] R. Benioub, M. Adnane, and K. Itaka, "Comparison study and simulation of the main multilevel inverter topologies for different output voltage levels," *International Journal on Electrical Engineering and Informatics*, vol. 9, no. 3, pp. 482–492, Sep. 2017.

[11] J. Li, G. Konstantinou, H. R. Wickramasinghe, and J. Pou, "Operation and control methods of modular multilevel converters in unbalanced AC grids: A review," *IEEE Journal of Emerging and Selected Topics in Power Electronics*, vol. 7, no. 2, pp. 1258–1271, Jun. 2019.

[12] M. P. Thakre, T. K. Jadhav, S. S. Patil, and V. R. Butale, "Modular multilevel converter with simplified nearest level control (NLC) strategy for voltage balancing perspective," in *2021 Innovations in Energy Management and Renewable Resources*, Kolkata, India, 2021.

[13] M. A. Kumar, A. K. Gopi, J. Biswas, and M. Barai, "A voltage balancing scheme for modular multilevel converter based on charge variation in each cycle," *IEEE Journal of Emerging and Selected Topics in Industrial Electronics*, vol. 2, no. 2, pp. 173–183, Apr. 2021.

[14] M. Tayyab and A. Sarwar, "Level shifted carrier-based pulse width modulation for modular multilevel converter," in *Lecture Notes in Electrical Engineering*, A. Iqbal, H. Malik, A. Riyaz, K. Abdellah, and S. Bayhan, Eds. Singapore: Springer, 2021, pp. 639–646.

[15] T. Kaliannan, J. R. Albert, D. M. Begam, and P. Madhumathi, "Power quality improvement in modular multilevel inverter using for different multicarrier PWM," *European Journal of Electrical Engineering and Computer Science*, vol. 5, no. 2, pp. 19–27, Apr. 2021.

[16] A. Dekka, B. Wu, and N. R. Zargari, "A novel modulation scheme and voltage balancing algorithm for modular multilevel converter," *IEEE Transactions on Industry Applications*, vol. 52, no. 1, pp. 432–443, Jan. 2016.

[17] J. Zhang, S. Shao, Y. Li, J. Zhang, and K. Sheng, "Arm voltage balancing control of modular multilevel resonant converter," *CES Transactions on Electrical Machines and Systems*, vol. 4, no. 4, pp. 303–308, Dec. 2020.

[18] F. Deng and Z. Chen, "Voltage-balancing method for modular multilevel converters switched at grid frequency," *IEEE Transactions on Industrial Electronics*, vol. 62, no. 5, pp. 2835–2847, May 2015.

[19] G. C. de Oliveira, G. Damm, R. M. Monaro, L. F. Lourenço, M. J. Carrizosa, and F. Lamnabhi-Lagarrigue, "Nonlinear control for modular multilevel converters with enhanced stability region and arbitrary closed loop dynamics," *International Journal of Electrical Power & Energy Systems*, vol. 126, Mar. 2021, Art. no. 106590.

[20] M. Ahmadijokani, M. Mehrasa, M. Sleiman, M. Sharifzadeh, A. Sheikholeslami, and K. Al-Haddad, "A back-stepping control method for modular multilevel converters," *IEEE Transactions on Industrial Electronics*, vol. 68, no. 1, pp. 443–453, Jan. 2021.

[21] R. Razani and Y. A.-R. I. Mohamed, "Fault-tolerant operation of the DC/DC modular multilevel converter under submodule failure," *IEEE Journal of Emerging and Selected Topics in Power Electronics*, vol. 9, no. 5, pp. 6139–6151, Oct. 2021.

[22] D. Karwatzki and A. Mertens, "Generalized control approach for a class of modular multilevel converter topologies," *IEEE Transactions on Power Electronics*, vol. 33, no. 4, pp. 2888–2900, Apr. 2018.

[23] K. Wang, L. Zhou, Y. Deng, Y. Lu, C. Wang, and F. Xu, "Application range analysis and implementation of the logic-processed CPS-PWM scheme based MMC capacitor voltage balancing strategy," *CPSS Transactions on Power Electronics and Applications*, vol. 4, no. 1, pp. 1–9, Mar. 2019.

[24] M. A. Perez, S. Ceballos, G. Konstantinou, J. Pou, and R. P. Aguilera, "Modular multilevel converters: Recent achievements and challenges," *IEEE Open Journal of the Industrial Electronics Society*, vol. 2, pp. 224–239, 2021.

[25] P. Hu, R. Teodorescu, S. Wang, S. Li, and J. M. Guerrero, "A currentless sorting and selection-based capacitor-voltage-balancing method for modular multilevel converters," *IEEE Transactions on Power Electronics*, vol. 34, no. 2, pp. 1022–1025, Feb. 2019.

[26] Y. Tang, L. Ran, O. Alatise, and P. Mawby, "Capacitor selection for modular multilevel converter," *IEEE Transactions on Industry Applications*, vol. 52, no. 4, pp. 3279–3293, Jul. 2016.

Sheik Hussain received the bachelor's degree in electrical and electronics engineering Anna University, Chennai, India in 2012 and the master's degree in Energy systems & management from Manipal Academy Higher Education, Dubai, The United Arab Emirates in 2022. At present, he holds the position of Overall Design coordinator and Site manager at Scan Electromechanical contract Co LLC, UAE and the 13-years' experience in the medium and high voltage substation & power plants.

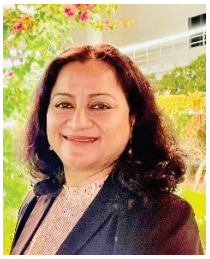

Roma Raina received her Ph.D. degree from Jamia Millia Islamia, New Delhi, India. She is an Associate Professor in the School of Engineering and IT with Manipal Academy of Higher Education Dubai Campus, The United Arab Emirates. Her research area focuses on the optimization of radial power distribution systems. She is holding a Masters & Bachelor's degree in Engineering in the field of Controls & Instrumentation and has about 25 years of teaching experience. She has published various papers in reputed journals & conference.

Hidayathullah Mohamed Ismail received the bachelor's degree in electrical and electronics engineering and the master's degree in power systems engineering from Anna University, Chennai, India in 2012 and 2015, respectively. He received his Ph.D. at the SRM Institute of Science and Technology, Kanchipuram, Tamil Nadu, India. His research interests include modular multilevel converters, control strategy for power converters applicable to HVDC system, power electronics converter for grid connected system, and DC-DC converters for renewable energy application.

Saravanan Kaliyaperumal received his B.E. degree in Electrical and Electronics Engineering from Alagappa Chettiar College of Engineering and Technology, Madurai Kamaraj University, Karaikudi, Tamil Nadu, India in 1998. He received his M.E. degree in Power Electronics and Drives from Anna University, Guindy Campus, Chennai, Tamil Nadu, India in 2001. He completed his PhD degree in Jawaharlal Nehru Technological University, Kakinada, Andhra Pradesh, India in 2018. At present, he is an Associate Professor in Electrical and Electronics Engineering, SRM Institute of Science and Technology, Kattankulathur, Tamil Nadu, India. He has published several technical papers in national and international journals. His current research interests include Renewable Energy Systems, Electric Vehicles, and multilevel inverter. He is a Fellow of FIE, a Life Member of ISTE, and a Life member of SESI.